MODELING AND SIMULATION OF A HYDROMECHANICAL FLIGHT CONTROL SERVO ACTUATOR SYSTEM USING BOND-GRAPHS

Luciana Sayuri Mizioka, luciana_sayuri@hotmail.com
Luiz Carlos Sandoval Góes, goes@ita.br
Instituto Tecnológico de Aeronáutica, Praça Marechal Eduardo Gomes 50, Cep 12228-900, São José dos Campos, São Paulo, Brazil

Abstract. *In this paper it is presented a bond-graph model of a hydromechanical system for flight control actuation. The nonlinear characteristics of the servo actuator such as the effects associated to aerodynamic loads in the commanded surface and the hinge moment associated with nonlinear friction, among other nonlinearities, can influence the aircraft control system performance. The dynamic modeling of these effects is important in system development to attend the specified flight control requirements. The system model is described and simulated using the bond-graph language, which is a generalized graphical description of the dynamic system aimed to represent the energy exchange between physical system components belonging to different physical domains.*

Keywords*: servo actuator, servo valve, hydraulic fluid, bond-graphs*

1. INTRODUCTION

To survive among a competitive market, a company shall be capable to innovate in a shorter period, increasing the quality and test security, and costs reduction. The aerospace industry is an example of competitive market, which requires a continuous product development improvement. The aircraft manufacturers and their suppliers have been exploring the systems models simulation, glimpsing a reduction of special tests. It allows the manufacturers to develop theirs products in an economical way and in a reduced period of time, using the expensive tests just for products performance validation, such as flight tests.

The modeling method has been applied to several aircraft systems, including flight controls systems. When applicable, there are some important aspects that shall be taken into account as real hydromechanical system effects e.g. orifice flow for laminar and turbulent conditions [Borutzky, Barnard and Thoma, 2002], pressure fluctuation in hydraulic pipes [Higo, Yamamoto, Tanaka, Sakurai and Nakada, 2000], variable orifice flow [Viall, Zhang, 2000], system performance under different types of fire resistant fluids [Dasgupta, Chattapadhyay, Mondal, 2005], nonlinearities related to servo actuator [Joshi, 2005]. Some of these effects have already been analyzed in laboratory tests, contributing to modeling community.

The system designer shall have a complete knowledge of the selected hydraulic fluid properties as well as its effects, in respect to the compatibility between the hydraulic components and fluid as o-rings and the compliance of the system dynamic behavior and considering the system nonlinearities and the environment it will operate.

The study consists on investigating the hydromechanical actuator system performance under hydraulic fluid temperature variation, considering all the servo actuator nonlinearities, comparative study on how the hydraulic fluids affect system dynamic response [Mizioka, 2009].

2. PROBLEM FORMULATION

Figure 1 presents the schematic of a flight control system described in [Gritti, 2004], considering a hydromechanical servo actuator.

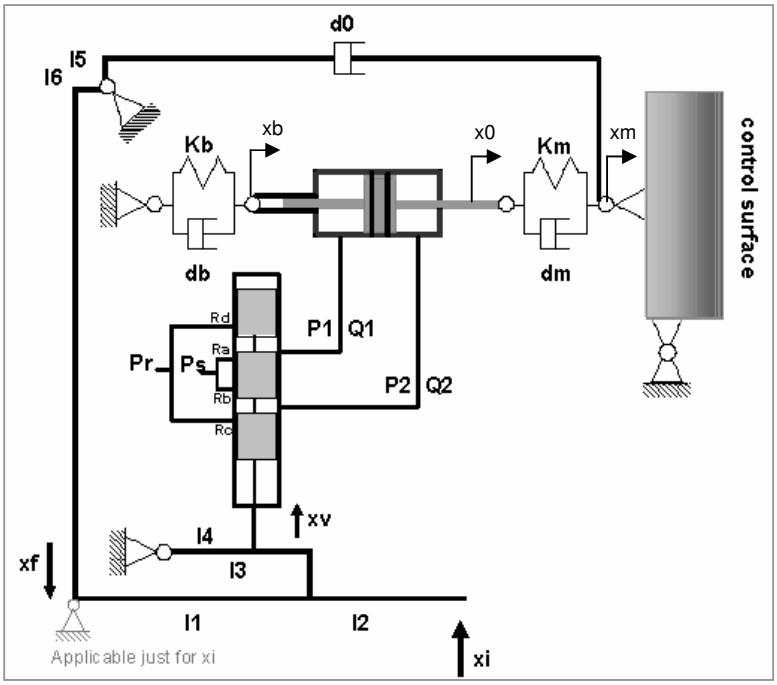

Figure 1 Schematic of a flight control system.

From Fig. 1, it is observed that the system is composed by mechanical and hydraulic components as levers mechanism, hydraulic servo valve, hydraulic actuator and a control surface.

Fig. 2 shows the bond-graph representation of the actuator kinematics. The command action reaches the input lever (xi), which is transmitted through the 0, 1 and TF junctions, displacing it to up or down (xv). This transmission ratio is given by Eq. (1).

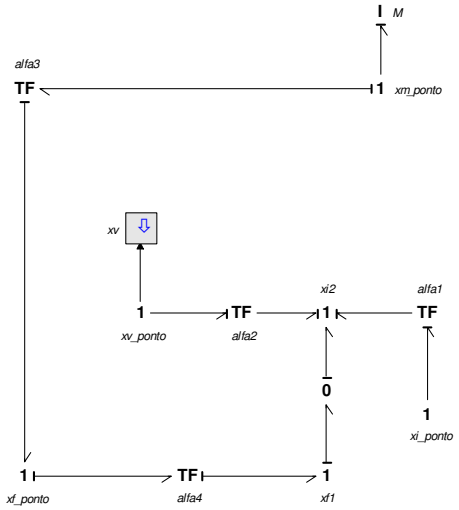

Figure 2 Valve actuation mechanism representation through bond-graphs

$$xv = \frac{l1}{l1+l2} * \frac{l4}{l3} * xi \tag{1}$$

where:

l1, l2, l3, l4: titanium levers [m]
xi: input displacement [m]
xv: valve spool displacement [m]

Figure 3 shows the bond-graph representation of the four-way srvo valve. The valve spool displacement modulates the valve orifices restrictions opening, which is represented by four modulated resistors. Each different pressurte is represented by a 0 junction. One port is fed with hydraulic fluid at the supply pressure (Ps) generated by the Hydraulic Power Generation System, the other one is connected to the return line, with pressure (Pr). The control ports , are connected to the actuator ports (P1, P2). The fluid flow is represented by 1 junctions and is controlled by the modulated resistances Ra, Rb, Rc and Rd, which are functions of xv. When the valve spool is centralized, there is no flow and the modulated resistances are infinite. When the valve spool moves up, (xv) is positive and the modulated resistances Ra and Rc become finite, allowing the fluid flow to pass through the orifices as expressed by Eq. (2) (Qa) and Eq. (4) (Qc). On the other hand, the modulated resistances Rb and Rd become infinite, there is no fluid flow. The inverse can be applied to the valve when its spool moves down, (xv) is negative and the modulated resistances Rb and Rd become finites, allowing the fluid flow pass through the orifices (1 junctions) as expressed by Eq. (3) (Qb) and Eq. (5) (Qd). On the other hand, the modulated resistances Ra and Rc become infinite, there is no fluid flow. The flow equations were modeled based on Borutzky, Barnard and Thoma, 2002, which considers orifice flow for laminar and turbulent conditions. The fluid viscosity and density are properties that affect the fluid flow and depend on the temperature and pressure.

The clearances leakage in the servo valve design is acceptable and represented by $Gleak.\Delta P/\nu$ but it shall be limited by the design requirement in order to maintain the system performance [Bizarria, 2009].

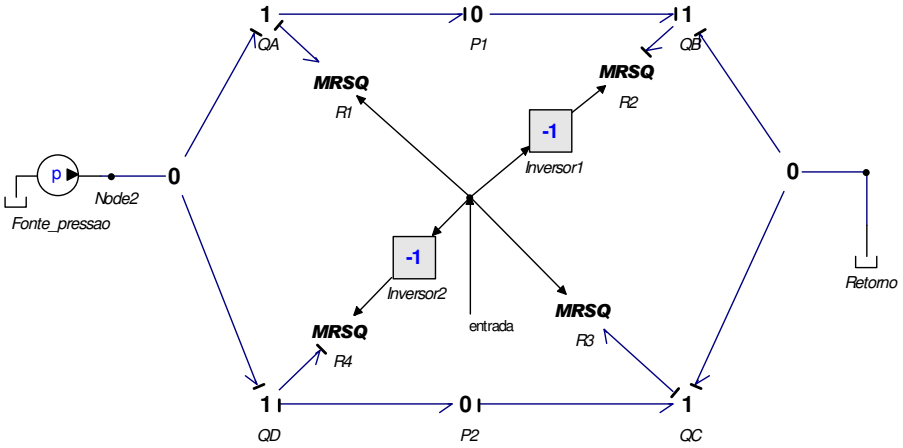

Figure 3 Valve representation through bond-graphs

$$Qa = \left(cturb * w * xv * \sqrt{\frac{2}{\rho} * |Ps - P1| + \left(\frac{\nu * Rt}{4 * cturb * w} \right)^2} - xv * \nu * \frac{Rt}{4} \right) * sign(Ps - P1) + Gleak \frac{.(Ps - P1)}{\nu} \tag{2}$$

for xv > 0

$$Qb = \left(cturb * w * xv * \sqrt{\frac{2}{\rho} * |P1 - \mathrm{Pr}| + \left(\frac{\nu * Rt}{4 * cturb * w} \right)^2} - xv * \nu * \frac{Rt}{4} \right) * sign(P1 - \mathrm{Pr}) + Gleak. \frac{(P1 - \mathrm{Pr})}{\nu} \tag{3}$$

for xv < 0

$$Qc = \left(cturb * w * xv * \sqrt{\frac{2}{\rho} * |P2 - \mathrm{Pr}| + \left(\frac{\nu * Rt}{4 * cturb * w} \right)^2} - xv * \nu * \frac{Rt}{4} \right) * sign(P2 - \mathrm{Pr}) + Gleak. \frac{(P2 - \mathrm{Pr})}{\nu} \tag{4}$$

for xv > 0

$$Qd = \left(cturb * w * xv * \sqrt{\frac{2}{\rho} * |Ps - P2| + \left(\frac{\nu * Rt}{4 * cturb * w} \right)^2} - xv * \nu * \frac{Rt}{4} \right) * sign(Ps - P2) + Gleak. \frac{(Ps - P2)}{\nu} \tag{5}$$

for xv < 0

where:

Qa, Qb, Qc, Qd: flow through orifice [m^3/s]
cturb: =0.61 discharge coefficient applied to high Reynolds values
w: area gradient [m^2/m]
ρ: fluid density [kg/m^3]
ν: kinematics viscosity [m^2/s]
Rt:=9.33 [Borutzky, Barnard, Thoma, 2002, p. 146]
Ps: forward pressure [Pa]
Pr: return pressure [Pa]
P1, P2: valve pressure [Pa]
Gleak: laminar leakage conductance in the valve clearances

Figure 4 shows the bond-graph of the piston movement model that is powered by the pressure difference between actuator chambers (C1 and C2 elements) over the piston area (TF junctions) as presented in Eq. (6). In the same way, it is reduced by non-linear forces as friction between the cylinder and piston [Kuster, 1996], and collision force between the actuator cylinder strokes and piston area given by Eq. (7), Eq. (8) and Eq. (9). The reaction forces given by mechanic connection between the piston lever and surface rod kinematics reflect in the piston movement, reducing the piston force.

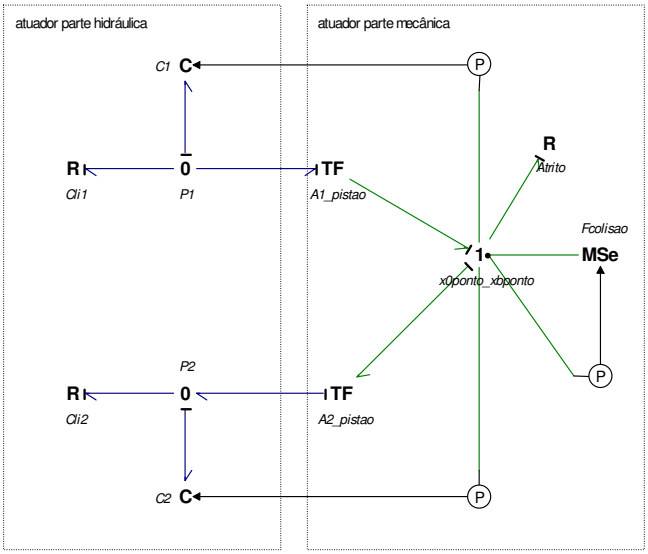

Figure 4 Actuator representation through bond-graphs

$$Mp * \ddot{x}0 = Ap * PL - Km * (x0 - xm) - dm * (\dot{x}0 - \dot{x}m) - Ffriction + Fcol \tag{6}$$

$$Ffriction = Fc * \tanh(slope * (\dot{x}0 - \dot{x}b)) + dv * (\dot{x}0 - \dot{x}b) \tag{7}$$

$$Fcol = -Kc * (x0 - xb) - dc * \min([(\dot{x}0 - \dot{x}b), 0]) \tag{8}$$

for $x0 - xb < stroke$, stroke< 0

$$Fcol = -Kc * ((x0 - xb) - stroke) - dc * \max([(\dot{x}0 - \dot{x}b), 0]) \tag{9}$$

for $x0 - xb > stroke$, stroke > 0

$$PL = P1 - P2 \tag{10}$$

where:

Mp: piston mass [kg]
Ap: piston area [m2]
PL: pressure difference between actuator chambers [Pa]

Ffriction: friction forces between cylinder and piston [N]
Fc: static friction coefficient [N/m]
Slope: friction Coulomb slope
dv: viscous friction coefficient [N.s/m]
Fcol: collision force [N]
Kc: actuator piston and cylinder stiffness [N/m]
dc: actuator piston and cylinder damping [N.s/m]
stroke: actuator cylinder length [m]
x0: piston displacement [m]
xb: actuator cylinder displacement [m]
$\dot{x}0$: piston speed [m/s]
$\dot{x}b$: actuator cylinder speed [m/s]
Km: rigidez da conexão atuador superfície [N/m]
db: amortecimento do atuador estrutura [N.s/m]
dm: amortecimento do atuador superfície [N.s/m]
$\ddot{x}0$: piston acceleration [m^2/s]

The flow through the actuator is given by Eq. (11). It considers the actuator internal and external leakages and the nonlinearities related to fluid compressibility.

$$QL = Ap*(\dot{x}0 - \dot{x}b) + \frac{V}{\beta}*\dot{P}L + Cli*PL \tag{11}$$

where:

Ap: piston area [m^2]
Cli: actuator internal and external leakage coefficient [m^3/s/Pa]
β: bulk modulus [Pa]
QL: flow through the actuator [m3/s]
V: hydraulic fluid volume [m3]
$\dot{P}L := \frac{dPL}{dt}$ load pressure varying in time [Pa/s]

The actuator cylinder model is represented by Eq. (12) and is powered by its mechanical connection with the aircraft structure as structure stiffness and connection damping. The equation also considers reaction forces generated by piston movement and its nonlinearities.

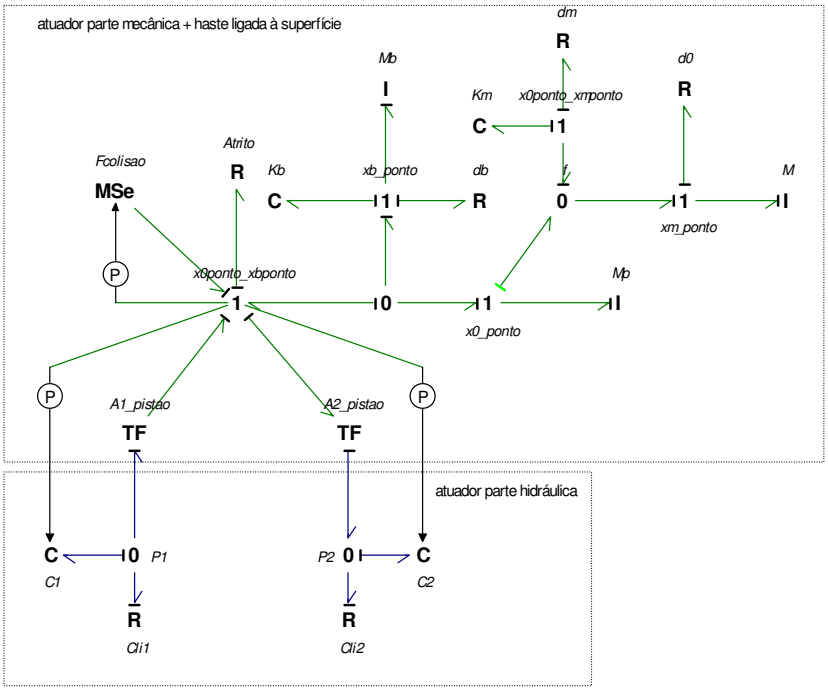

Figure 5 Surface actuation mechanism representation through bond-graphs

$$Mb * \ddot{x}b = -Ap * PL + Kb * xb + db * \dot{x}b + Ffriction - Fcol \tag{12}$$

where:

Mb: actuator cylinder mass [kg]
Kb: actuator structure connection stiffness [N/m]
db: actuator structure connection damping [N.s/m]
xb: actuator cylinder displacement [m]
$\dot{x}b$: actuator cylinder speed [m/s]
$\ddot{x}b$: actuator acceleration [m^2/s]

For the surface model, it has not been considered the kinematics between the piston rod and the surface. It was simplified in order to reduce it to a mass load connected to piston rod. Equation (13) considers the mass dynamic related to the structure connection as stiffness and damping.

$$M * \ddot{x}m = Km * (x0 - xm) + dm * (\dot{x}0 - \dot{x}m) - d0 * \dot{x}m \tag{13}$$

where:

M: load mass [kg]
$\ddot{x}m$: surface acceleration [m^2/s]

The surface movement displaces the feedback levers mechanism, which will be summed to the input command, modifying the valve spool position, described by the Eq. (14).

$$xv = \frac{l2}{l1 + l2} * \frac{l4}{l3} * \frac{l6}{l5} * xm \tag{14}$$

where:

l5, l6: titanium levers [m]

Equation (1) and Eq. (15) are simplified to:

$$xv = ki.xi - kf.xm \tag{15}$$

where:

$$ki = \frac{l1}{l1 + l2} * \frac{l4}{l3} \tag{16}$$

$$kf = \frac{l2}{l1 + l2} * \frac{l4}{l3} * \frac{l6}{l5} \tag{17}$$

Figure 6 shows the bond-graph of the complete hydromechanical servo actuator system.

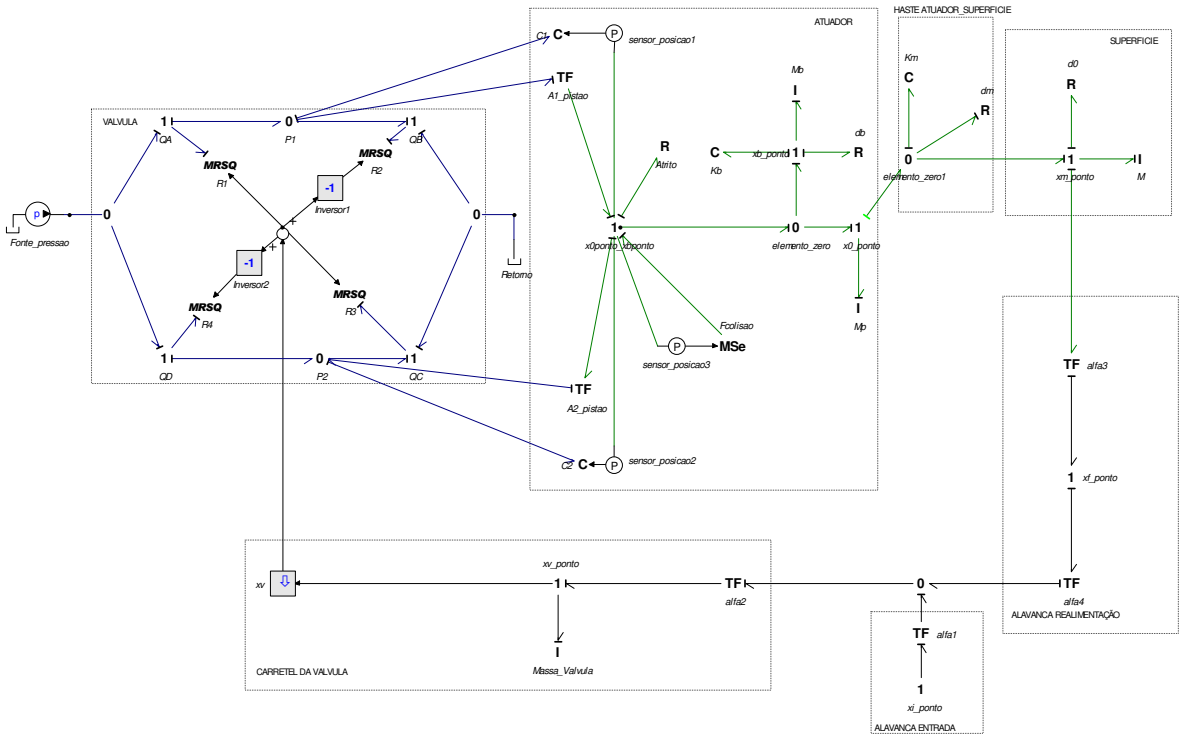

Figure 6 Hydromechanical servo actuator system representation through bond-graphs

3. CASES SIMULATONS

The studies are based on the hydromechanical system's characteristics, whose parameters are presented in Appendix A Table A, evaluating the hydraulic fluid temperature that influence the rod displacement. It has been generated some systems models, by changing the hydraulic fluid properties, as bulk modulus, density and kinematics viscosity.

The system model is simulated in closed loop, considering a step as a reference equivalent to a rudder pedal deflection of 9 degrees. This signal is summed to the feedback signal resulting in the valve spool displacement as shown in Fig. 2, that controls the valve restriction, by opening or closing it. In this case study the valve opens suddenly and closes as soon as the piston actuator reaches the cylinder stroke, which is connected to a rod that reflects the piston final position as well as its speed, presented by Fig. 7 and Fig. 8. This process controls the orifice opening allowing the fluid flows through the valve and the cylinder, generating pressure difference between the cylinder actuator chambers as shown in Fig. 9 and Fig. 10.

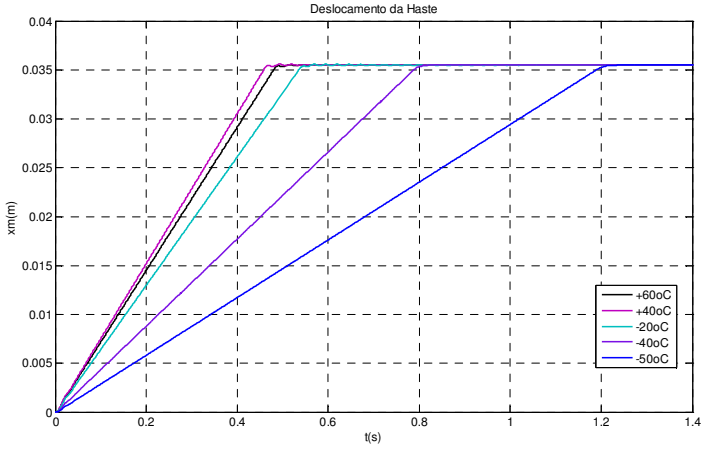

Figure 7 Rod position under hydraulic fluid temperature variation

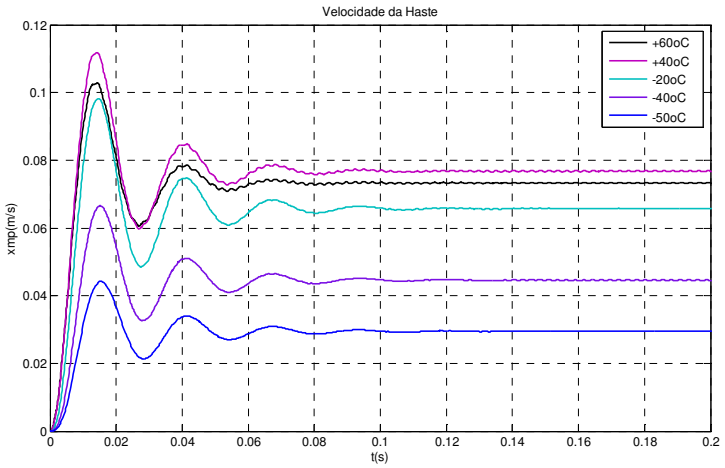

Figure 8 Rod speed under hydraulic fluid temperature variation

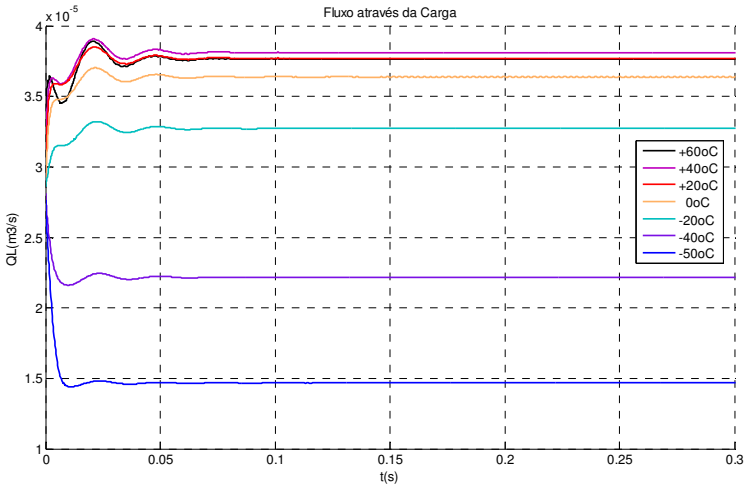

Figure 9 Fluid flow under hydraulic fluid temperature variation

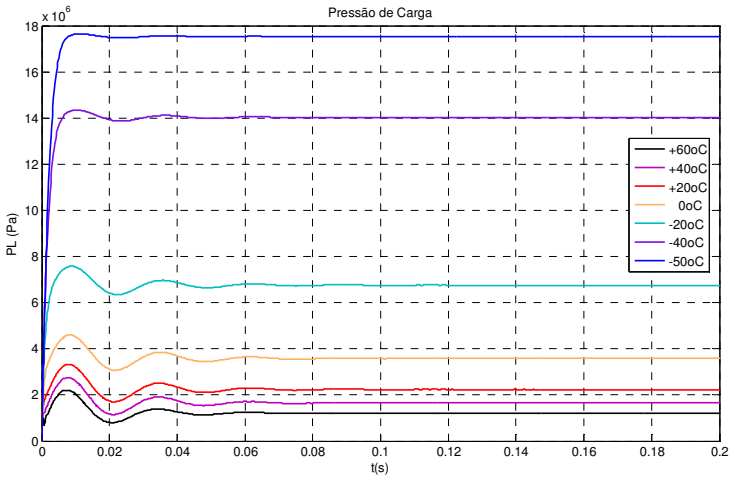

Figure 10 Load pressure under hydraulic fluid temperature variation

In Fig. 7, it shows that for temperatures below -40ºC the rod movement raise time increases significantly when compared to the rise times for -20ºC, +40ºC e +60ºC. It happens due to the influence of fluid temperature, because for low temperatures it becomes thicker, with the density and viscosity increase. In this case to move the piston rod, it´s

necessary a higher pressure difference as presented in Fig. 10. As the flow and the speed are directly linked, the low flow means low speed, requiring more time to have a piston rod response.

In Fig. 9, it can be observed that the flow curves do not present a linear ratio with the temperature, neither the space between the curves, neither the transitory signals accomplish homogenously the temperature variation.

This system behavior difference is due to the fluids properties, since the other parameters are all the same for the three models.

4. CONCLUSION

The present study evaluates the dynamic system response for a hydromechanical servo actuator system. The study presents the modeling through bond-graphs as well as its mathematical formulation considering the real system effects such as fluid compressibility, viscous and friction damping and servo valves nonlinearities. As simulation result, it was shown that the hydraulic fluid temperature affects the dynamic system, in order to not have the design requirements accomplished. It is really important to have a temperature study during product development.

For future studies it is recommended to consider a change of physical properties of the hydraulic fluid due to trapped air evaluating the bulk modulus and system performance, improvements applied to the actuator model.

APPENDIX A

Table A Data used for simulation

Parameter	Value	Unit	Description
ki	0.2591	-	Coefficient for input signal
kf	2.496	-	Feedback coefficient
Mb	1.0	kg	Actuator cylinder mass
Kb	3.40×10^{6}	N/m	Actuator structure stiffness
db	0.00	N.s/m	Actuator structure damping
Kc	1.0×10^{7}	N/m	Stiffness during colision with cylinder stroke
dc	1.0×10^{4}	N.s/m	Damping during colision with cylinder stroke
stroke	35.6×10^{-3}	m	Cylinder stroke
Fc	123	N/m	static friction coefficient
slope	1000	-	Coulomb friction slope
dv	3.40×10^{8}	N.s/m	Slip friction
Mp	3.5	kg	Piston mass
Km	1.98×10^{7}	N/m	Actuator surface stiffness
dm	0.0	N.s/m	Actuator surface damping
d0	1043.26	N.s/m	Structure damping
M	45.00	kg	Surface mass
A1_pistão, A2_pistão	4.9×10^{-4}	m^2	Piston area
Ps	20.7×10^{6}	Pa	supplied pressure
Pr	0.00	Pa	Return pressure
Cli1, Cli2	5.0×10^{-17}	$m^3/s/Pa$	Actuator leakage coefficient
Rt	9.33	-	Transition Reynolds
cturb	0.61	-	Discharge coefficient for high Reynolds values
Cd	0.61	-	Discharge coefficient
xmax	2.0×10^{-3}	m	Maximum valve spool module (xv)
Gleak	1.4×10^{-17}	$m^3/s/Pa$	Valve leakage coefficient

5. REFERENCES

1. Bizarria, C. O., 2009. “Prognóstico de Falhas no Atuador do Leme da Aeronave Embraer-190”, Masters Thesis – Instituto Tecnológico de Aeronáutica, São José dos Campos. (Msc. Thesis)
2. Borutzky, W., Barnard, B. and Thoma, J., 2002. “An Orifice Flow Model for Laminar and Turbulent Conditions”, Simulation Modeling Practice and Theory, p.141-152.

3. Dasgupta, K.; Chattapadhyay, A.; Mondal, S. K., 2005 "Selection of Fire Resistant Hydraulic Fluids Through System Modeling and Simulation". Simulation Modelling Practice and Theory, p.1-20.
4. Green, W. L., 1985. "Aircraft Hydraulic Systems: An Introduction to the Analysis of Systems and Components". Great Britain: John Wiley & Sons Ltd, 137p.
5. Gritti, M., 2004. "Especificação da Arquitetura e Análise de Desempenho de um Sistema de Leme", Masters Thesis – Instituto Tecnológico de Aeronáutica, São José dos Campos.
6. Higo, H., Yamamoto, K., Tanaka, K., Sakurai, Y., Nakada, T., 2000. "Bondgraph Analysis on Pressure Fluctuatio in Hydraulic Pipes**".** Industrial Electronics Society, 2000. IECON 2000. 26th Annual Confjerence of the IEEE**.**
7. Joshi, A., 2005. "Modelling of Flight Control Hydraulic Actuators Considering Real System Effects". Engineering Simulators Uses and Techniques III, AIAA-2005-6297.
8. Kuster, H. E. 1996. "Projeto e Análise de um Servo Atuador Hidromecânico para Aplicação Aeronáutica**",** Masters Thesis – Instituto Tecnológico de Aeronáutica, São José dos Campos.
9. Merrit, H. E., 1967. "Hydraulic Control Systems". New York: John Wiley & Sons Inc.
10. Mizioka, L. S., 2009. "Modelagem e análise de desempenho do servo atuador do sistema de leme de uma aeronave sob variação de temperatura", Masters Thesis – Instituto Tecnológico de Aeronáutica, São José dos Campos.
11. Viall, E. N., Zhang, Q., 2000. "Determining the Discharge Coefficient of a Spool Valve". Proceedings of American Control Conference. Chicago, Illinois.

6 RESPONSIBILITY NOTICE

The authors are the only responsible for the material included in this paper.